



ELSEVIER

Available online at www.sciencedirect.com

SCIENCE @ DIRECT®

Physica A 351 (2005) 523–550

PHYSICA A

www.elsevier.com/locate/physa

Passive motion in dynamical disorder as a model for stock market prices

James P. Gleeson*

Department of Applied Mathematics, University College Cork, Ireland

Received 7 July 2004; received in revised form 25 November 2004

Available online 6 January 2005

Abstract

A new model for stock price fluctuations is proposed, based upon an analogy with the motion of tracers in Gaussian random fields, as used in turbulent dispersion models and in studies of transport in dynamically disordered media. Analytical and numerical results for this model in a special limiting case of a single-scale field show characteristics similar to those found in empirical studies of stock market data. Specifically, short-term returns have a non-Gaussian distribution, with super-diffusive volatility. Assuming a power-law decay of the time correlation of the disorder, the returns correlation decays rapidly but the correlation function of the absolute returns exhibits a slow power-law decay. The returns distribution converges towards Gaussian over long times. Some important characteristics of empirical data are not, however, reproduced by the model, notably the scaling of tails of the cumulative distribution function of returns. Implied volatilities for options pricing are found by numerical simulation.
© 2004 Elsevier B.V. All rights reserved.

PACS: 05.60.-k; 89.65.Gh; 05.40.-a; 02.50.-r

Keywords: Stock market dynamics; Random-walk models

*Tel.: +353 21 490 3410; fax: +353 21 427 0813.

E-mail address: j.gleeson@ucc.ie (J.P. Gleeson).

1. Introduction

Random fluctuations in stock market prices have long fascinated investors and mathematical modelers alike. Although the investors' hopes of accurately predicting tomorrow's share price appear to be in vain, models which limit themselves to statistical characteristics such as distributions and correlations have had some success. Bachelier's classical model [1] treats the stock price $S(t)$ as a random walk, leading to the conclusion that the distribution of prices is Gaussian. Samuelson [2] instead describes the log-price

$$x(t) = \ln[S(t)/S(0)] \quad (1)$$

as a random walk, and therefore concludes that the stock price $S(t)$ should have a log-normal distribution. This model remains in common usage, despite the shortcomings listed below, not least because it permits the derivation of an equation for pricing options and other financial derivatives, e.g., the famous Black–Scholes equation [3]. Nevertheless, empirical evidence from stock market data indicates that the random walk model inadequately describes many important features of the stock price process. The following stylized facts are accepted as established by these studies [3,4]:

- (i) Short-term returns are non-Gaussian, with 'fat tails' and high central peaks. The center of the returns distribution is well fitted by Lévy distributions [5]. Recent studies indicate that the tails of the returns distribution decay as power-laws [6]. As the lag time increases, the returns distributions slowly converge towards Gaussian; recent analysis of the Standard & Poor 500 index (S&P500) estimates this convergence is seen only on lags longer than 4 days [6].
- (ii) The correlation function of returns decays exponentially over a short timescale, consistent with market efficiency. However, the correlation function of the *absolute value* of the returns shows a much slower (power-law) decay [6].
- (iii) The volatility (standard deviation of returns) grows like that of a diffusion (random walk) process, i.e., as the square root of the lag time, for lag times longer than about 10 min. However, higher frequency (shorter lag) returns demonstrate a super-diffusive volatility, which can be fitted to power-laws with exponents found to range between 0.67 and 0.77 [6,7].
- (iv) The distribution of stock price returns exhibits a simple scaling: in Ref. [5] a power-law scaling of the peak of the returns distribution $P(0)$ with lag time is shown to hold across many magnitudes of lag times. The exponent of the power-law is approximately -0.7 .

Most of the references cited here examine data from the Standard & Poor 500 index (S&P500), but other international markets are found to behave similarly [6].

The predictions of the random-walk model can be investigated using the random differential equation

$$\frac{dx}{dt} = u_w(t), \tag{2}$$

which yields the log price $x(t)$ from each realization of the random function $u_w(t)$. The classical random walk follows from taking $u_w(t)$ to be a Gaussian white-noise process with zero mean and (auto)correlation function [8]:

$$\langle u_w(t)u_w(t') \rangle = \alpha^2 \delta(t - t'), \tag{3}$$

where $\delta(t)$ is the Dirac delta function, and the angle brackets denote averaging over time or over an ensemble of realizations. White noise is the formal derivative of a Wiener process, which connects (2) to rigorous methods for stochastic differential equations [9]. Note that throughout this paper all stochastic processes are assumed (unless explicitly stated otherwise) to have zero mean and to be statistically stationary.

Eq. (2) is easily solved, and leads to results which do not agree with the empirical facts (i)–(iv) listed above. Defining the return on the stock price $S(t)$ at time t as the forward change in the logarithm of $S(t)$ over the lag time Δ :

$$\begin{aligned} r_\Delta(t) &= x(t + \Delta) - x(t) \\ &= \ln S(t + \Delta) - \ln S(t), \end{aligned} \tag{4}$$

it is found that the white-noise case leads to probability distribution functions (PDFs) for r_Δ which are Gaussian at all lags Δ , in contrast to (i). The lack of memory effects in white-noise leads to correlation functions which decay immediately to zero, unlike (ii). The volatility grows diffusively for all lag values, and so has no super-diffusive range, while the scaling of $P(0)$ follows a power-law different from that found for actual prices, see (iv) above.

A natural generalization of the white-noise model again takes a form similar to (2)

$$\frac{dx}{dt} = u_c(t), \tag{5}$$

but with $u_c(t)$ now being a non-white or colored process, incorporating some memory effects. For the particularly simple case of Gaussian noise, it can be described fully by its correlation function

$$\langle u_c(t)u_c(t') \rangle = \alpha^2 R(t - t'). \tag{6}$$

Here $R(t)$ decays from a maximum of unity at $t = 0$ to zero as $t \rightarrow \infty$, and α^2 is the variance of the process u_c . Gaussian noise is attractive because it appears naturally as the limiting sum of many independent noise sources under the central limit theorem [8], and because of its analytical tractability. Indeed Eq. (5) is again easily solvable for Gaussian u_c , but leads once more to Gaussian-distributed returns at all lag times, in contrast to (i). Moreover, the correlation of absolute returns does not decay more slowly than the returns correlation, as required by (ii).

These failings of simple differential equation models have inspired many attempts to reproduce the empirical facts (i)–(iv) using various stochastic models. As a sample of just a few of these, we list the truncated Lévy flights model [10,11], ARCH and GARCH models [12,13], non-Gaussian Ornstein–Uhlenbeck processes [14], and a model based on a continuous superposition of jump processes [15,7]. The first three of these were reviewed in Ref. [16]. An ideal model should reproduce all the experimental facts (i)–(iv), by giving a simple picture of the stochastic process underlying the stock price time series, but no model has yet been found which fulfills all these criteria [17].

In this paper we examine the results of generalizing the random walk models (2) and (5) to motion in a random field:

$$\frac{dx}{dt} = u(x, t). \quad (7)$$

Here $u(x, t)$ is a Gaussian random field with zero mean, which is fully described by its correlation function

$$\langle u(x, t)u(x', t') \rangle = \alpha^2 Q(x - x', t - t') \quad (8)$$

$$= \alpha^2 S(x - x')R(t - t'). \quad (9)$$

For simplicity we take the field to be homogeneous and stationary; the factorization in (9) of the correlation into separate time- and x -correlations is for ease of exposition only, and more complicated inter-dependent correlations can be considered. The averaging procedure in Eq. (8) is over an ensemble of realizations of the random field u , or using a uniform measure over all possible (x, t) values.

Eq. (7) implies that the log-price $x(t)$ changes in a random fashion, but the rate of change is randomly dependent on both time and the current value of x . Note that random-walk models (2) and (5) may be recovered by taking $S(x) \equiv 1$ and choosing the time correlation $R(t)$ appropriately. We will show that the x -dependence in the noise term yields qualitatively different results to the random walk models, and that many of the empirical observations (i)–(iv) of stock markets may be reproduced by (7).

The x -dependent noise term in (7) is motivated by recent studies in turbulent dispersion [18] and transport in dynamically disordered media [19]. These investigations employ Eq. (7), but with a rather different interpretation: $x(t)$ is the position vector (in 2 or 3 dimensions) of a passive tracer, and $u(x, t)$ is the velocity vector field which transports the tracer. The tracer is called *passive* because it is assumed not to affect the velocity field by its presence, and so $u(x, t)$ is a prescribed random field. An instructive example is the motion of a small buoy on the surface of the ocean [20]: the two-dimensional vector $x(t)$ then describes the position of the buoy (by its longitude and latitude, say) while the tracer is moved by the ocean waves according to (7), with the Gaussian field $u(x, t)$ providing an approximate description of the ocean wave field.

The distribution of such tracers resulting from motion in a Gaussian field is known to be non-Gaussian, at least over short to intermediate timescales [18,21]. Crucial to

understanding this effect is the difference between the *Eulerian* velocity $u(x, t)$, i.e., the velocity measured at the fixed location x at time t , and the *Lagrangian* velocity

$$v(t) = u(x(t), t), \quad (10)$$

which is the time series of velocity measurements made by the tracer itself as it moves through the random field [22]. When there is no x -dependence in the velocity field u , the Eulerian and Lagrangian velocities coincide, but otherwise a Gaussian Eulerian velocity field can yield non-Gaussian Lagrangian processes. The relationship between Eulerian and Lagrangian random processes is an active research area, especially in the case of a compressible (non-zero divergence) velocity field which is of interest here [23–25].

Our model of the log-price uses a scalar “position” $x(t)$ and “velocity” $u(x, t)$ rather than the vector-valued analogues in the turbulent dispersion problems described above. Nevertheless, the concept of Eulerian and Lagrangian velocities carries over to the one-dimensional case, and so we will refer to $x(t)$ as the “price tracer”, with its “velocity” $u(x, t)$ related by Eq. (7). The fact that the Eulerian velocity field $u(x, t)$ is Gaussian allows us to obtain analytical results, and may be justified as a consequence of the central limit theorem applied to the sum of many independent agents trading in the stock.

The remainder of this paper is structured as follows. In Section 2 the consequences of the x -dependence of the noise in Eq. (7) are examined through some simple examples, and a special limiting case (single-scale field) is highlighted. Results from the theory of Gaussian disorder are used to derive the x -dependence of the noise from a simple model of trader behavior. The statistics of the Lagrangian velocity (10) in the single-scale case are found analytically in Sections 3 and 4, and are related to the statistics of the returns r_A . Numerical simulations of Eq. (7) are considered in Section 5, and a simple method for generating Monte Carlo time series in the single-scale case is found. Results from such simulations are presented in Section 6, and compared to the stylized facts (i)–(iv), as presented in Refs. [6,5]. The implied volatility for pricing of options is calculated, leading to volatility ‘smiles’. Section 7 comprises of discussion of the results and directions for future work.

2. x -dependent velocity fields

The concept of x -dependence in the velocity of the log-price $x(t)$ was introduced in Section 1. To gain some intuitive understanding of the effect of such x -dependence, we first return to the random walk model with colored noise $u_c(t)$, independent of x , as in (5) and (6):

$$\frac{dx}{dt} = u_c(t), \quad \text{with } \langle u_c(t)u_c(t') \rangle = \alpha^2 R(t - t'). \quad (11)$$

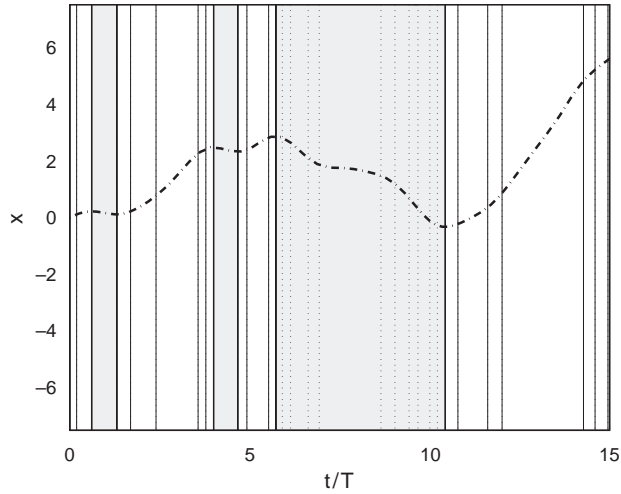


Fig. 1. Motion of a stock tracer in a random field which depends only on time, as in (5). Shaded areas and dotted contour lines indicate negative values of $u_c(t)$.

For clarity, we consider in this section a specific form for the time correlation $R(t)$:

$$R(t) = \exp\left(-\frac{t^2}{2T^2}\right), \tag{12}$$

where a characteristic decay time T has been introduced. Fig. 1 shows the contours of a single realization of the x -independent $u_c(t)$, negative values of the velocity being denoted by shaded areas and dotted contour lines. Time increases along the horizontal axis, with the stock log price x measured on the vertical axis. The motion of a stock tracer with initial condition $x(0) = 0$ is shown also; note the negative rate of change of stock price in the shaded regions (negative velocity), and the positive rate of change in the regions where $u > 0$. Because there is no x -dependence in (11), the velocity field depends only on time, and so the contours are vertical lines. By contrast, a simple x -dependent velocity field of the type proposed in (7) has a non-trivial x -correlation function $S(x)$ in Eq. (9); for example in Fig. 2 we use

$$S(x) = \exp\left(-\frac{x^2}{2l^2}\right), \tag{13}$$

where l defines a correlation scale ($l \rightarrow \infty$ recovers the x -independent case). The contours in Fig. 2 display a more complicated structure than in Fig. 1, and this is reflected in the observed motion of the stock prices. The three parameters α , T and l characterizing the random field may be combined into one dimensionless quantity

$$\varepsilon = \frac{l}{\alpha T}, \tag{14}$$

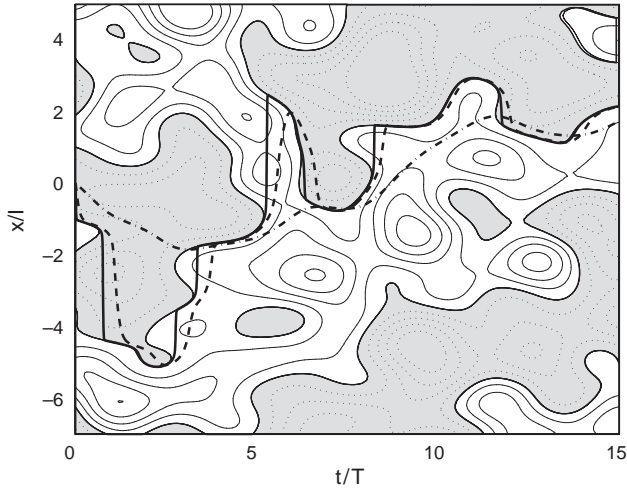


Fig. 2. Motion of stock tracers in a random field which depends on both time and x , as in (7). The correlation functions are (12) and (13), and the values of ε are: $\varepsilon = 1.0$ (dash-dotted), $\varepsilon = 0.1$ (dashed), and $\varepsilon = 0.01$ (solid).

and if the time, log price and velocity are re-scaled using these parameters:

$$\begin{aligned}
 t &= T\tilde{t}, \\
 x &= l\tilde{x}, \\
 u &= \alpha\tilde{u},
 \end{aligned}
 \tag{15}$$

then the equation of motion (7) becomes

$$\varepsilon \frac{d\tilde{x}}{d\tilde{t}} = \tilde{u}(\tilde{x}, \tilde{t}).
 \tag{16}$$

Note that the re-scaled velocity field \tilde{u} has unit variance. In Fig. 2 the stock price motions resulting from solving (16) are shown for ε values of $\varepsilon = 1$, $\varepsilon = 0.1$, and $\varepsilon = 0.01$. When ε is large, the length scale l of the randomness in x is much larger than the effect αT of the random variation in time—this is analogous to the case of weak space dependence in turbulent dispersion problems studied in Ref. [18] using perturbation theory. In the case of $\varepsilon \gg 1$, small deviations of the stock price distribution from a Gaussian shape are found, with kurtosis less than 3. However, the studies of empirical data mentioned in Section 1 indicate that the kurtosis of stock returns is much larger than 3, and so the weakly space-dependent theory does not seem relevant here.

The opposite limit, i.e., $\varepsilon \ll 1$ appears more promising. In Fig. 2, we observe that the stock prices for parameter values $\varepsilon = 0.1$ and 0.01 display some interesting generic features. Constrained by the equation of motion to move downwards in shaded regions (where the velocity \tilde{u} is negative), and upwards in unshaded regions, the stock tracers tend to become trapped near curves of $\tilde{u} = 0$, with \tilde{u} positive below them and negative above them. These stable positions disappear when the

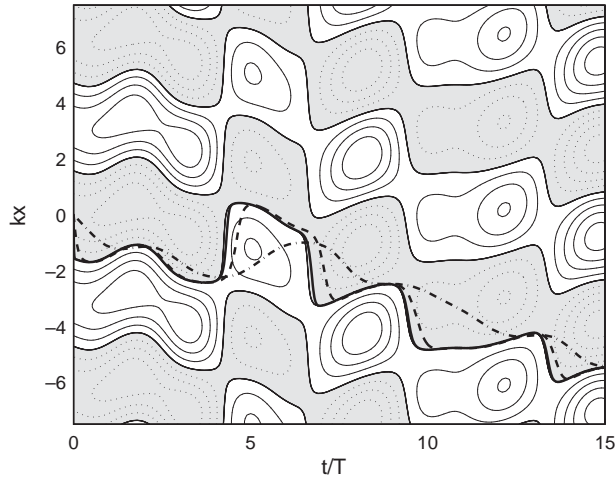


Fig. 3. Motion of stock tracers in a single-scale random field with x -correlation function given in Eq. (17). See Fig. 2 for description of line types.

zero-velocity manifold ‘folds over’, and the stock tracer is then driven by Eq. (16) to move quickly to another slow manifold. A complete understanding of the dynamics of the system as $\epsilon \rightarrow 0$ requires a singular perturbation approach [27] to Eq. (16), but the important feature for our work is the following of the zero-velocity manifold by the stock tracer, punctuated by fast jumps.

An analytical approach to the general $\epsilon \rightarrow 0$ case has not yet been found, but some interesting features are highlighted by choosing a particularly simple form for the x -correlation function:

$$S(x) = \cos(kx), \tag{17}$$

where k is a constant. This correlation function corresponds to a so-called ‘single-scale’ Gaussian velocity field, which (as shown in Ref. [28]) can always be written in the form

$$u(x, t) = f(t) \cos(kx) + g(t) \sin(kx), \tag{18}$$

where $f(t)$ and $g(t)$ are independent Gaussian random functions of time, each with zero mean, variance α^2 , and a given correlation function $R(t)$:

$$\langle f(t)f(t') \rangle = \langle g(t)g(t') \rangle = \alpha^2 R(t - t'). \tag{19}$$

An example of motion in such a single-scale field is shown in Fig. 3. Note the periodicity in the vertical direction, and the lack of jumps. In the remainder of this paper we will concentrate on this simplified example and show that many of the statistical characteristics of the resulting stock returns are remarkably similar to those observed in empirical data.

2.1. Agent models

In this section we show how the market model (7) can be attributed to the actions of heterogeneous traders making up the market. Our aim here is not a realistic model of trader psychology, but rather to demonstrate that the x -dependence of Eq. (7) can be derived from more fundamental assumptions, and so motivate our work in the remainder of this paper on the consequences of the random field model.

Consider a market for a given financial instrument (e.g. a stock) made up of N trading agents, with quantities scaled so that finite results can be found in the limit $N \rightarrow \infty$. Let $\phi_v(x, t)$ be the supply/demand function of agent v , which is negative when the agent can supply the instrument at price x at time t , and positive when the agent is demanding the instrument. The crucial feature of this model is that each agent’s supply or demand depends not only on time, but also upon the current price of the stock. For instance, consider an agent who wishes to sell stock at (or near) a target price x_v , and who can trade only during his lunch break, i.e., at times close to t_v . The corresponding $\phi_v(x, t)$ is negative in the vicinity of $x = x_v$ and for times t close to t_v , but is zero for other values of x and t , since the agent is unwilling to sell at prices other than the preset target price, and can trade only within a finite time window. Thus $\phi_v(x, t)$ has compact support in the two-dimensional (x, t) space.

The simplest model of the effects of the supply and demand of individual agents upon the stock price is

$$\frac{dx}{dt} = d(x, t) - s(x, t) = \sum_v \phi_v(x, t), \tag{20}$$

where $d(x, t)$ is the total demand at price x and time t , and $s(x, t)$ is the corresponding total supply. According to the previous discussion, d and s are composed of agents with positive and negative ϕ_v , respectively. This model then links the velocity field used in Eq. (7) to the total supply/demand of the agents:

$$u(x, t) = \sum_v \phi_v(x, t). \tag{21}$$

Clearly the statistical properties of $u(x, t)$ can now be related to those of the ϕ_v functions. An instructive example is the case where all agents share a common ‘pulse shape’ h in their supply/demand functions

$$\phi_v(x, t) = a_v h(x - x_v, t - t_v). \tag{22}$$

Here the supply/demand function of agent v is described by an amplitude a_v (the sign of which determines whether the agent is supplying or demanding stock), individual target prices and times x_v and t_v , and a compact pulse shape $h(x, t)$ which is common to all agents. Treating the (x, t) space by analogy with a two-dimensional disordered material allows us to apply results from the theory of Gaussian disorder in the $N \rightarrow \infty$ limit, see for example [29]. If the pulses making up the field (21) have uniform density in the (x, t) space, the resulting field $u(x, t)$ is a homogeneous, stationary, Gaussian field of mean $\langle a_v \rangle$ (taken to be

zero here), and variance

$$\alpha^2 = N \langle a_v^2 \rangle \int_{-\infty}^{\infty} \int_{-\infty}^{\infty} h^2(x', t') dx' dt' . \quad (23)$$

The correlation function (8) of the field is

$$\langle u(0, 0)u(x, t) \rangle = N \langle a_v^2 \rangle \int_{-\infty}^{\infty} \int_{-\infty}^{\infty} h(x', t') h(x' + x, t' + t) dx' dt' . \quad (24)$$

For example, an ensemble of agents who allow some flexibility (of order l) in their target prices, and flexibility of order T in their trading times can be modelled using the pulse shape

$$h(x, t) = \exp\left(-\frac{x^2}{l^2}\right) \exp\left(-\frac{t^2}{T^2}\right) . \quad (25)$$

This choice yields a random field with correlation function (9), where $R(t)$ and $S(x)$ are as in Eqs. (12) and (13). Fig. 2 shows a sample realization of such a field.

The single-scale field (17) may also be generated by agents with a separable h function, with sinusoidal variation in the x -direction, and a pulse shape in the t -direction chosen to give the desired $R(t)$ (see Section 5). The resulting sinusoidal variation of ϕ_v with x is a rather artificial trading strategy, and it is thus unlikely that single-scale fields accurately describe real market dynamics. Nevertheless it is possible to obtain analytical results in the $\varepsilon \rightarrow 0$ limit of this case, which we believe reflect many of the important features of more complicated fields, and so we concentrate in this paper on the single-scale case.

3. Lagrangian velocity and PDF

In this section we consider the statistical characterization of motion along the $u = 0$ curves of the single-scale random field (18), according to the equation of motion (7), and with the Gaussian random functions $f(t)$ and $g(t)$ defined as in (19). Again, the analogue with tracer motion on the surface of a turbulence ocean proves instructive. The Eulerian velocity at a point x at time t is defined by the random field (18). Each tracer particle moving through this field will, however, experience its own time history of velocity variations; this is called the Lagrangian velocity of the tracer $v(t)$. The crucial point in our use of random-field models of stock price motion is that the Eulerian field may, as in (18), have Gaussian statistics, while the Lagrangian velocity (that is, the velocity ‘felt by the tracer’) need not be Gaussian. Some intuitive notion of why this might be may be gained from considering the fact that the velocity at space-time points (x, t) picked at random from the Eulerian field has a Gaussian distribution; on the other hand, the dynamics of the tracer particles mean that they are more likely to cluster in regions of low velocity, with high-velocity transitions between, meaning both zero values of v and high values are more likely than for a Gaussian distribution. This argument holds for any random field, but as we show in this section, a quantitative description may be derived in the case of a single-scale field (17) for the $\varepsilon \rightarrow 0$ limit.

In the limit of small ε , we saw in the previous section that the stock tracer motion is confined to curves with $u = 0$. While the Eulerian velocity on these curves is zero by definition, the Lagrangian velocity is non-zero, as the tracer moves to remain on the $u = 0$ curve. In fact, the Lagrangian velocity felt by the particle trapped on such a curve is given by

$$v(t) = - \frac{\frac{\partial u}{\partial t} \Big|_{u=0}}{\frac{\partial u}{\partial x} \Big|_{u=0}}, \tag{26}$$

with the derivatives evaluated on the curve $u = 0$. For the single scale field (18), an explicit expression for the Lagrangian velocity may be found in terms of the functions $f(t)$ and $g(t)$ and their derivatives:

$$v(t) = \frac{1}{k} \frac{fg' - gf'}{f^2 + g^2}. \tag{27}$$

When the Lagrangian velocity $v(t)$ is known, the equation of motion for the tracer is simply

$$\frac{dx}{dt} = v(t), \tag{28}$$

with solution

$$x(t) = x(0) + \int_0^t v(t') dt'. \tag{29}$$

Similarly, the return on the stock over a time lag of Δ is given by

$$\begin{aligned} r_\Delta(t) &= x(t + \Delta) - x(t) \\ &= \int_t^{t+\Delta} v(t') dt'. \end{aligned} \tag{30}$$

Clearly the statistics of the returns follow from the statistics of the Lagrangian velocity, indeed for short time lags it might be expected from (30) that

$$r_\Delta(t) \approx v(t)\Delta, \tag{31}$$

so that the distribution of returns, for instance, can be related directly to the distribution of the Lagrangian velocity. We shall see later that (31) is not fully accurate for large values of v , but the Lagrangian velocity distribution will still prove extremely useful.

To find the probability distribution function $P(v)$ of the Lagrangian velocity, we first consider the cumulative probability that the Lagrangian velocity v at a given time is greater than some chosen value V . Assuming initially that $g < 0$, Eq. (27) then implies that $v > V$ if and only if

$$f' > - \frac{f^2 + g^2}{g} kV + \frac{gf}{g} \equiv F, \tag{32}$$

where we use the symbol F to denote the right-hand side. Since f, g, f' and g' are independent Gaussian random variables at any single moment in time, we denote their PDFs by P_f, P_g etc., and the cumulative probability of the event (32) for $g < 0$ is

$$C_{g < 0}(V) = \int_{-\infty}^0 dg \int_{-\infty}^{\infty} df \int_{-\infty}^{\infty} dg' \int_F^{\infty} df' P_g P_f P_{g'} P_{f'} . \tag{33}$$

The PDF of v then follows from

$$\begin{aligned} P_{g < 0}(v) &= - \frac{d}{dV} C(V) \Big|_{V=v} \\ &= \int_{-\infty}^0 dg \int_{-\infty}^{\infty} df \int_{-\infty}^{\infty} dg' P_g P_f P_{g'} P_{f'} \Big|_{f'=F} \frac{\partial F}{\partial V} \Big|_{V=v} , \end{aligned} \tag{34}$$

and the fact that

$$\frac{\partial F}{\partial V} = k \frac{f^2 + g^2}{|g|} . \tag{35}$$

An identical argument gives a similar result in the case $g > 0$. Noting that the variances of f' and g' both equal $-\alpha^2 R''(0) = \alpha^2 / \tau_0^2$, where we introduce the notation τ_0 for the timescale defined by the initial radius of curvature of the function R :

$$\tau_0 = \frac{1}{\sqrt{-R''(0)}} , \tag{36}$$

the integrations over the f - g plane may be performed by using polar coordinates $f = r \cos \theta, g = r \sin \theta$, yielding

$$\begin{aligned} P(v) &= \int_{-\infty}^{\infty} dg \int_{-\infty}^{\infty} df P_g P_f \frac{k\tau_0}{\sqrt{2\pi\alpha^2}} \sqrt{f^2 + g^2} \exp \left[-(f^2 + g^2) \frac{k^2 \tau_0^2 v^2}{2\alpha^2} \right] \\ &= \frac{k\tau_0}{2[1 + k^2 \tau_0^2 v^2]^{3/2}} . \end{aligned} \tag{37}$$

The PDF (37) of the Lagrangian velocity $P(v)$ is symmetric in v , and so has mean zero. Note that the tails of $P(v)$ decay as $|v|^{-3}$ for large $|v|$, so the variance of v does not exist. Also, (37) effectively contains only one free parameter $k\tau_0$, and is otherwise independent of the choice of correlation function $R(t)$ for f and g .

4. Correlation of Lagrangian velocity and returns

The (normalized) correlation of the stock returns with lag Δ , at time t , is defined by averaging the product of the returns at times separated by τ :

$$\frac{\langle r_{\Delta}(t)r_{\Delta}(t + \tau) \rangle}{\langle r_{\Delta}(t)^2 \rangle} , \tag{38}$$

and for stationary returns becomes independent of t . The correlation is normalized by the variance $\langle r_{\Delta}(t)^2 \rangle$ of the returns at lag Δ , which is known as the

squared volatility [6]. In this section we derive analytical results to show how the volatility and the returns correlation for a single-scale field with $\varepsilon \rightarrow 0$ depend on the time correlation function $R(t)$ of the Eulerian field, and on α and k .

Because of the dependence (30) of the returns on the Lagrangian velocity, the correlation of the returns can be written in terms of the correlation function of v :

$$\begin{aligned} \langle r_\Delta(t)r_\Delta(t + \tau) \rangle &= \int_t^{t+\Delta} dt_1 \int_{t+\tau}^{t+\tau+\Delta} dt_2 \langle v(t_1)v(t_2) \rangle \\ &= \int_0^\Delta dt_1 \int_\tau^{\tau+\Delta} dt_2 \langle v(t_1)v(t_2) \rangle \\ &= \int_0^\Delta dt_1 \int_\tau^{\tau+\Delta} dt_2 L(t_1 - t_2) \end{aligned} \tag{39}$$

$$= \int_0^\Delta (\Delta - t_1)[L(t_1 - \tau) + L(t_1 + \tau)] dt_1, \tag{40}$$

where we have used the stationarity of the returns, and defined the Lagrangian velocity correlation function

$$L(t_1 - t_2) = \langle v(t_1)v(t_2) \rangle. \tag{41}$$

Note the Lagrangian velocity is assumed to be a stationary process—this has not been proven to follow from Eulerian stationarity in the general case [23], but appears to hold in numerical simulations. We will proceed to calculate $L(t)$, and then use (40) to find the volatility and returns correlation. We note here that when the separation time τ is much larger than the lag Δ , the returns covariance (40) is approximated by

$$\langle r_\Delta(t)r_\Delta(t + \tau) \rangle \sim \Delta^2 L(\tau), \tag{42}$$

consistent with (31).

The correlation function of the stationary random process v is written as an eight-dimensional integral, using the definition (27) of the Lagrangian velocity:

$$\begin{aligned} L(t) &= \langle v(0)v(t) \rangle \\ &= \frac{1}{k^2} \int \dots \int \frac{f_1 g'_1 - g_1 f'_1}{f_1^2 + g_1^2} \frac{f_2 g'_2 - g_2 f'_2}{f_2^2 + g_2^2} P_{12}(f_1, f'_1, f_2, f'_2) \\ &\quad \times P_{12}(g_1, g'_1, g_2, g'_2). \end{aligned} \tag{43}$$

Here the eight-fold integrals are over f, g, f' and g' evaluated at each of the two times $t = 0$ (with subscript 1) and $t = t$ (subscript 2). The random functions f and g are independent of each other, but the joint probability functions for f and its derivative at different times is found from the Gaussian joint PDF

$$P_{12}(\mathbf{w}) = \frac{1}{(2\pi)^2} (\text{Det } \mathbf{A})^{1/2} \exp \left[-\frac{1}{2} \mathbf{w}^T \mathbf{A} \mathbf{w} \right] \tag{44}$$

for the vector of arguments, $\mathbf{w} = (f_1, f'_1, f_2, f'_2)$, with a similar expression for g . The matrix \mathbf{A} is defined by

$$A_{ij}^{-1} = \langle w_i w_j \rangle \tag{45}$$

and when written out in full:

$$\mathbf{A}^{-1} = \alpha^2 \begin{pmatrix} 1 & 0 & R(t) & R'(t) \\ 0 & -R''(0) & -R'(t) & -R''(t) \\ R(t) & -R'(t) & 1 & 0 \\ R'(t) & -R''(t) & 0 & -R''(0) \end{pmatrix}. \tag{46}$$

Using (44) and (46) in (43) enables us to calculate the Lagrangian correlation $L(t)$. We briefly describe here the steps in the calculation of the multi-dimensional integrals. First, the four integrals over the variables f'_1, g'_1, f'_2, g'_2 are performed—the dependence of the integrand on each of these variables is linear, so the Gaussian integrals may be calculated straightforwardly. For the remaining four variables, we transform to polar coordinates in the (f_1, g_1) and (f_2, g_2) planes:

$$f_1 = r \cos \theta, \quad g_1 = r \sin \theta, \quad f_2 = \rho \cos \phi, \quad g_2 = \rho \sin \phi. \tag{47}$$

The ϕ integral is then trivial, and by integrating over $\theta, r,$ and $\rho,$ the final result emerges:

$$L(t) = \frac{1}{2k^2 R(t)^2} \{R(t)R''(t) - R'(t)^2\} \log[1 - R(t)^2]. \tag{48}$$

Eq. (48) gives an explicit formula for the Lagrangian velocity correlation in terms of the time correlation $R(t)$ of the single-scale Eulerian field. When the function $R(t)$ is given, $L(t)$ follows immediately from (48), and hence the volatility and returns correlation can be calculated using (40). Before examining the results for the returns, we consider the limiting forms of $L(t)$ for small and large arguments.

Assuming that $R(t)$ is sufficiently smooth near $t = 0$ to allow the definition of τ_0 as in Eq. (36), a small-time expansion of (48) yields

$$L(t) \sim -\frac{1}{2k^2 \tau_0^2} \log\left(\frac{t^2}{\tau_0^2}\right) \text{ as } t \rightarrow 0. \tag{49}$$

Note this diverges as t approaches zero, so the variance of the Lagrangian velocity does not exist, in accord with our conclusion at the end of Section 3.

For large time arguments, we are particularly interested in power-law decays of correlations, and so consider how the decay of $R(t)$ influences that of $L(t)$. Taking a power-law decay with exponent $-\beta$:

$$R(t) \sim t^{-\beta} \text{ as } t \rightarrow \infty, \tag{50}$$

the corresponding Lagrangian correlation is found from (48) to decay as

$$L(t) \sim -\frac{\beta}{2k^2} t^{-2\beta-2} \text{ as } t \rightarrow \infty. \tag{51}$$

The negative sign here indicates that the Lagrangian correlation approaches zero from below at large times, being negative whenever $R(t)$ has a power-law decay.

The squared volatility is found by setting $\tau = 0$ in (40):

$$\text{vol}^2(\Delta) = \langle r_\Delta(t)^2 \rangle = 2 \int_0^\Delta (\Delta - t)L(t) dt. \tag{52}$$

For short lags, with $\Delta \ll \tau_0$, it follows from (49) that the volatility may be approximated by

$$\text{vol}^2(\Delta) \approx \frac{1}{2k^2} \frac{\Delta^2}{\tau_0^2} \left[3 - \log\left(\frac{\Delta^2}{\tau_0^2}\right) \right] + O\left(\frac{\Delta^4}{\tau_0^4}\right). \tag{53}$$

Note that while this expression limits to zero as Δ vanishes, it does not follow a simple power law in Δ because of the logarithmic term. Although empirical stock volatilities have been fitted with power-laws [6,7], we show in the next section that (53) can also match the data quite well.

For large time lags Δ , empirical data shows a linear growth in vol^2 with Δ . From (52), we can find an expression for the rate of change of vol^2 with Δ :

$$\frac{d}{d\Delta} \text{vol}^2(\Delta) = 2 \int_0^\Delta L(t) dt, \tag{54}$$

and hence conclude that the squared volatility grows linearly with Δ for large lags if the integral

$$\int_0^\infty L(t) dt \tag{55}$$

has a finite positive value. Assuming a power-law form of $R(t)$ for large arguments, we use the result (51) for the asymptotic form of $L(t)$. It immediately follows that the integral (55) is finite if $\beta > -\frac{1}{2}$, and hence at large lags the squared volatility grows linearly with Δ in this case.

In empirical stock data, correlations of nonlinear functions of the returns often display significantly slower decay than the correlations of the returns themselves. One quantity of interest is the correlation of absolute returns, which, using (31), may be related to the correlation of absolute Lagrangian velocities (for short lags) as

$$\langle |r_\Delta(t)||r_\Delta(t + \tau)| \rangle - \langle |r_\Delta(t)^2| \rangle \approx \Delta^2 \{ \langle |v(t)v(t + \tau)| \rangle - \langle |v(t)^2| \rangle \}. \tag{56}$$

Following similar procedures as in the calculation of $L(t)$, it can be shown that the large- t asymptotics corresponding to a power-law $R(t) \sim t^{-\beta}$ give a correlation of absolute Lagrangian velocities scaling as

$$\langle |v(0)v(t)| \rangle - \langle |v^2| \rangle \sim t^{-2\beta}. \tag{57}$$

In contrast to (51), this correlation remains positive at large times; note too that its rate of decay is slower than that of (51).

Before proceeding to numerical simulations, we briefly summarize the theoretical results. We have obtained the PDF of the Lagrangian velocity in

(37), and related the Lagrangian velocity correlation $L(t)$ to the given Eulerian correlation $R(t)$ in (48). This permits estimates of the volatility as a function of lag. Finally, we expect a power-law scaling for the absolute returns correlation when $R(t)$ has a power-law decay. In the following sections we perform numerical simulations to confirm and extend these results.

5. Numerical simulations

To extend the analytical results found in the previous section, we consider the implementation of numerical simulations of motion in random fields. Random fields $u(x, t)$ may be generated using standard techniques [30], with the ordinary differential equation (7) being solved using Runge–Kutta methods. Averages may be calculated over an ensemble of realizations, or over a long time series $x(t)$ in a single realization, to closely mimic the statistical analysis of S&P 500 data performed in Refs. [5,6].

A random field with zero mean and correlation function (9) may be generated using a superposition of random Fourier modes [30]:

$$u(x, t) = \frac{1}{\sqrt{N}} \sum_{n=1}^N A_n \cos(\omega_n t + k_n x) + B_n \sin(\omega_n t + k_n x), \quad (58)$$

with the amplitudes A_n and B_n chosen from independent Gaussian distributions of zero mean and variance α^2 . The ω_n and k_n are chosen from distributions of random numbers chosen so as yield the correlation (9). Specifically, the ω_n are chosen from a distribution shaped as the Fourier transform of $R(t)$, with the distribution of the k_n being the Fourier transform of $S(x)$. Thus, Gaussian distributions with zero mean and unit variance are used for the ω_n and k_n to generate the random field of Fig. 1, as the Fourier transforms yield $R(t) = \exp(-t^2/2)$ and $S(x) = \exp(-x^2/2)$ as required in Eqs. (12) and (13).

For the special case of a single-scale field considered here, the k_n are all $\pm k$, and the field may be written in the simpler form (18), see Ref. [28]. Accordingly we only require a method for generating the random functions of time $f(t)$ and $g(t)$, and this is easily derived from (58):

$$f(t) = \frac{1}{\sqrt{N}} \sum_{n=1}^N A_n \cos(\omega_n t) + B_n \sin(\omega_n t), \quad (59)$$

with a similar formula for $g(t)$. The A_n, B_n are chosen as above. We are especially interested in the effects of power-law correlations $R(t)$, so we choose the ω_n in (59) from the Gamma distribution [30]:

$$G(\omega) = \frac{T^\beta}{\Gamma(\beta)} \omega^{\beta-1} e^{-T\omega}. \quad (60)$$

Here $\Gamma(\beta)$ denotes the usual Gamma function. The Fourier transform of $G(\omega)$ is the correlation function $R(t)$ of f :

$$R(t) = \left(1 + \frac{t^2}{T^2}\right)^{-\beta/2} \cos\left[\beta \tan^{-1}\left(\frac{t}{T}\right)\right], \tag{61}$$

which decays as $R(t) \sim t^{-\beta}$ for $t \gg T$.

The methods described above are sufficient to simulate motion in a random field as described by (7), or equivalently by the rescaled equation (16), and indeed this is how the stock log curves in Figs. 1–3 are generated. However, in the idealized limit $\varepsilon \rightarrow 0$ considered in the previous sections, the tracer closely follows the contour $u = 0$. In this limit it is therefore not necessary to explicitly solve the differential equation to determine $x(t)$ in a single-scale field, as this can be determined from the implicit equation $u(x, t) = 0$. From (18) we immediately obtain

$$x(t) = \frac{1}{k} \tan^{-1}\left[-\frac{f(t)}{g(t)}\right] \tag{62}$$

for motion along the $u = 0$ contour. Given the expression (59) for $f(t)$ and $g(t)$, Eq. (62) then generates the time series $x(t)$. Some care must be taken to ensure continuity of $x(t)$ near times when $g(t) = 0$, but overall this method is a very efficient way to create a model time series for $x(t)$.

6. Numerical results

In this section we report the results of employing the algorithm (62) to generate a sample time series $x(t)$ corresponding to a single-scale field, with Eulerian time correlation function given by (61). Having decided upon a single-scale field and the $\varepsilon \rightarrow 0$ limit, so that the stock tracer follows contours of $u(x, t) = 0$, our remaining choices to fit empirical stock data is rather limited. We are free to choose the time correlation function $R(t)$ and the spatial scaling factor k ; note the standard deviation α of the random field has disappeared because we have take the limit $\varepsilon \rightarrow 0$.

Our choice for $R(t)$ is motivated by the empirical results such as those reported in Ref. [6], and by our analysis in previous sections. We have seen in Section 4 that the Lagrangian velocity correlation becomes negative, with a power-law decay exponent of $-2\beta - 2$ when $R(t)$ has a power-law decay exponent of $-\beta$. On the other hand, the correlation of absolute values of the velocity remains positive for large t , with a decay exponent -2β . Studies of the corresponding returns correlations in Ref. [6] have concluded that the correlation decays exponentially quickly to the noise level, whereas the absolute returns correlation exhibits a slow decay with power-law exponent of approximately $-\frac{1}{3}$. Matching this to our result (57) motivates us to choose a power-law form for $R(t)$ as given in (61), taking the value of $\beta = \frac{1}{6}$. The time-scaling T is chosen to be 10 min, to approximately match the volatility results of Ref. [6]. Having thus defined the function $R(t)$, we are left with only the single parameter k . This is chosen to be 500, to approximately fit the volatility results

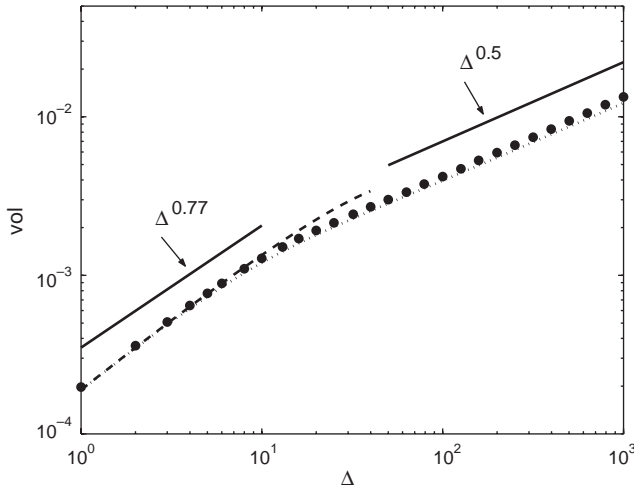


Fig. 4. Volatility of returns as a function of lag time Δ for time correlation $R(t)$ as in Eq. (61), with $\beta = \frac{1}{6}$ and $T = 10$ min. Symbols show the results of numerical simulation; dotted line is the analytical expression (52); dashed line is the small- Δ approximation (53); solid lines show power-laws with exponent 0.5 (large lags), and 0.77 (small lags), as fitted to empirical data in Ref. [7].

(see below) to those in Ref. [6]. These choices of correlation function and parameter values are used for all numerical simulations (Figs. 4 through 11).

Each realization consists of 1.6×10^6 values of $x(t)$, modelling the log price at 1-min intervals, to mimic the S&P500 data set used in Ref. [5]. Averaging is over time within each realization; we show results from different realizations only when statistical scatter is evident in the single-realization results. From the series for $x(t)$, it is straightforward to calculate the series of returns over integer time lags Δ

$$r_{\Delta}(t) = x(t + \Delta) - x(t) \tag{63}$$

and to calculate various statistical properties of the returns.

The volatility

$$\text{vol}(\Delta) = \sqrt{\langle r_{\Delta}(t)^2 \rangle} \tag{64}$$

found by numerical simulation is plotted as a function of the lag Δ in Fig. 4 (filled circles). The parameter k is chosen as $k = 500$, in order to closely match the empirical $\Delta = 1$ volatility value as shown in Fig. 3(c) of [6]. Also shown in Fig. 4 is the analytical result (52), plotted as a dotted line, which confirms that the numerical method closely reproduces the exact results of Section 4. The dashed line in Fig. 4 is the small-lag approximation (53), and shows that the super-diffusive region of volatility (for lags under 10 min) is well-matched by the logarithmic-corrected quadratic power law in Δ . Analysis of the empirical data frequently leads to fitting

the super-diffusive volatility with a power-law, with exponents in the range 0.67 [6] to 0.77 [7]. At longer lags ($\Delta > 10$), random walk behavior ($\text{vol} \sim \sqrt{\Delta}$) is observed in all studies, and reproduced in our model as shown following equation (55). The solid lines in Fig. 4 show power-law scalings, with exponents 0.77 (for $\Delta < 10$), and 0.5 (for $\Delta \gg 10$), which are found in Ref. [7] to match the S&P500 volatility. Clearly these scalings also match the results of our model quite well, indicating that the model predictions behave similarly to the empirical volatility curve. Indeed, our result (53) predicts that a log-corrected quadratic fit should be superior to the power-law fits used in Refs. [6,7]. Testing this prediction requires higher frequency analysis of the empirical market data.

The probability distribution function (PDF) of the one-minute returns, $r_1(t)$, is plotted in Fig. 5. Open circles are from numerical simulations, and are well-fitted by the Lagrangian velocity PDF (37), up to high returns values. Note the returns are normalized by their standard deviation $\sigma \equiv \text{vol}(1) = 2 \times 10^{-4}$. The Gaussian distribution with this standard deviation is plotted with the dotted line: note the higher-than-Gaussian central peak of the model results, and the fatter tails. Fig. 5 is remarkably similar to Fig. 2 of Ref. [5], which shows the one-minute returns PDF from the S&P500. Indeed, in Ref. [5] it is demonstrated that the empirical results are well-fitted near the center of the distribution by a Lévy stable distribution with index $\alpha = 1.4$, and so in Fig. 5 we also show this distribution (dashed line), with scale factor chosen to match the peak value of the numerical distribution. Comparison with Fig. 2 of Ref. [5] shows that our numerical simulation returns have a very similar distribution to the S&P500 data, at least within $\pm 10\sigma$.

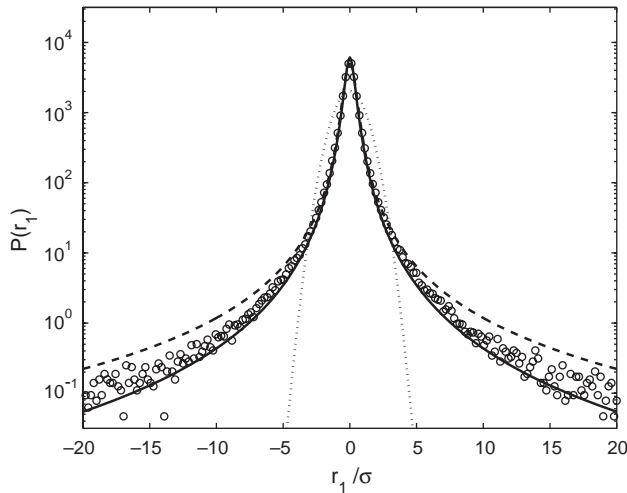


Fig. 5. Probability distribution function of 1-min returns from numerical simulation (symbols); $R(t)$ is as described in caption of Fig. 4. Dashed line is the Lévy distribution fitted to empirical data in Ref. [5]; solid line is the Lagrangian velocity PDF (37); dotted line is a Gaussian distribution with same variance as the data.

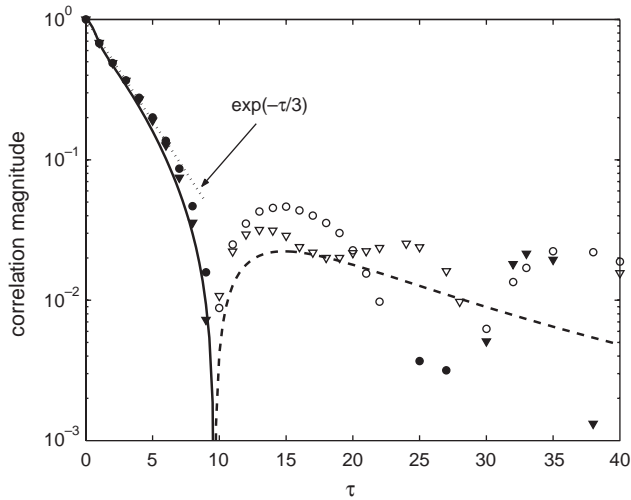


Fig. 6. Magnitude of the correlation function of 1-min returns, as a function of separation time τ ; $R(t)$ is as described in caption of Fig. 4. Numerical results from two realizations are shown (circles and triangles), with the analytical form (40) (solid and dashed lines). Negative correlation values are shown with open symbols and dashed line. The dotted line shows $\exp(-\tau/3)$ for comparison.

In Fig. 6 we consider the correlation function of the one-minute returns over a separation time τ , normalized by the volatility:

$$\frac{\langle r_1(t)r_1(t + \tau) \rangle}{\langle r_1(t)^2 \rangle}. \tag{65}$$

As this quantity has both positive and (small) negative values, we plot its absolute value on a log-linear scale. Statistical scatter causes some uncertainty in these numerical results, so the results of two different realizations (circles and triangles, respectively) are shown. According to (42) and (51), the returns correlation is negative for $\tau \gg 10$ min, which is confirmed by plotting the analytical result (40): this is shown as a solid line where the correlation is positive, and a dashed line where it is negative. The numerical simulation results match the analytical form well for $\tau < 10$ min, but degrade in quality when the correlation is negative. It is possible that more advanced numerical simulation methods such as Fourier-Wavelet [30] could alleviate this problem. Note filled symbols show positive numerical correlation values, with open symbols for negative values. The rapid decay of the correlation from $\tau = 0$ to 10 min is reminiscent of that found in S&P500 data, see Fig. 3(a) of Ref. [6] and Fig. 8(a) of Ref. [26]—we plot the function $\exp(-\tau/3)$ with a dotted line in Fig. 6 to show the similarity to an exponential decay. We note that the analytic expressions (40) and (48) do not readily imply such an exponential form for the decay; rather this (as with the power-law like behavior of the volatility) shows the ability of log-corrected Taylor series to mimic simpler functional forms. It is interesting that no assumption of exponential correlation decay needs to be built into

our model to reproduce this experimental observation. Unlike our model results, however, the empirical correlation does not exhibit negative values but instead reaches a “noise level” around 3×10^{-3} , where it flattens out without discernable structure. Our model suggests that it might be fruitful to search for evidence of negative correlations in the empirical data, which may currently be screened by the noise level.

The correlation function of the absolute value of one-minute returns (normalized to unity at zero separation) is

$$\frac{\langle |r_1(t)r_1(t + \tau)| \rangle - \langle |r_1(t)| \rangle^2}{\langle |r_1(t)|^2 \rangle - \langle |r_1(t)| \rangle^2} . \tag{66}$$

From empirical data, this is known to have a slow power-law decay with τ , with exponent of approximately $-\frac{1}{3}$, see Fig. 3(b) of Ref. [6] and Fig. 8(b) of Ref. [26]. The analytical result (57) for the present model indicates that a similar power-law form holds, indeed this is what motivated our choice of parameter $\beta = \frac{1}{6}$ in (61). Fig. 7 shows numerical results from two separate realizations (circles and triangles), with the solid line showing a power-law decay with exponent $-\frac{1}{3}$. The numerical correlations are all positive, but show a slight deviation from the expected power-law scaling. This may be related to the poor representation of the negative values of the returns correlation in Fig. 6. Comparison with empirical data (Fig. 3(b) of Ref. [6] and Fig. 8(b) of Ref. [26]) also shows that the model’s correlation decays faster than that of the S&P500 data for $\tau < 10$ min.

The non-Gaussian distribution of returns over longer time lags is examined in Figs. 8 and 9, using the methods applied to S&P500 data in Figs. 6–8 of Ref. [6]. The

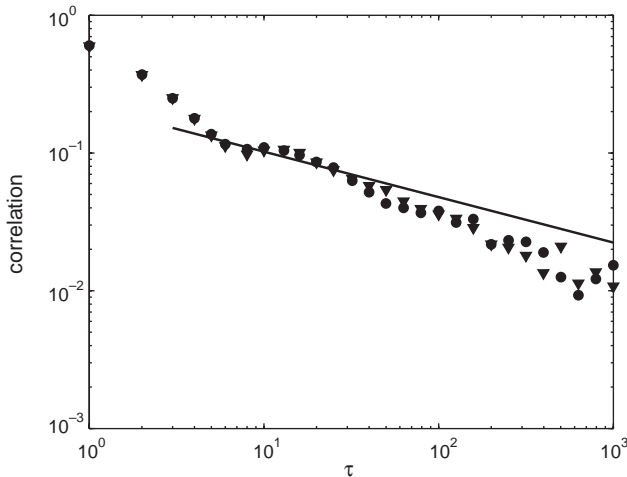


Fig. 7. Correlation function of absolute 1-min returns, as a function of separation time τ ; $R(t)$ is as described in caption of Fig. 4. Numerical results from two realizations are shown (circles and triangles). The solid line is a power-law scaling as (57), with parameter $\beta = \frac{1}{6}$.

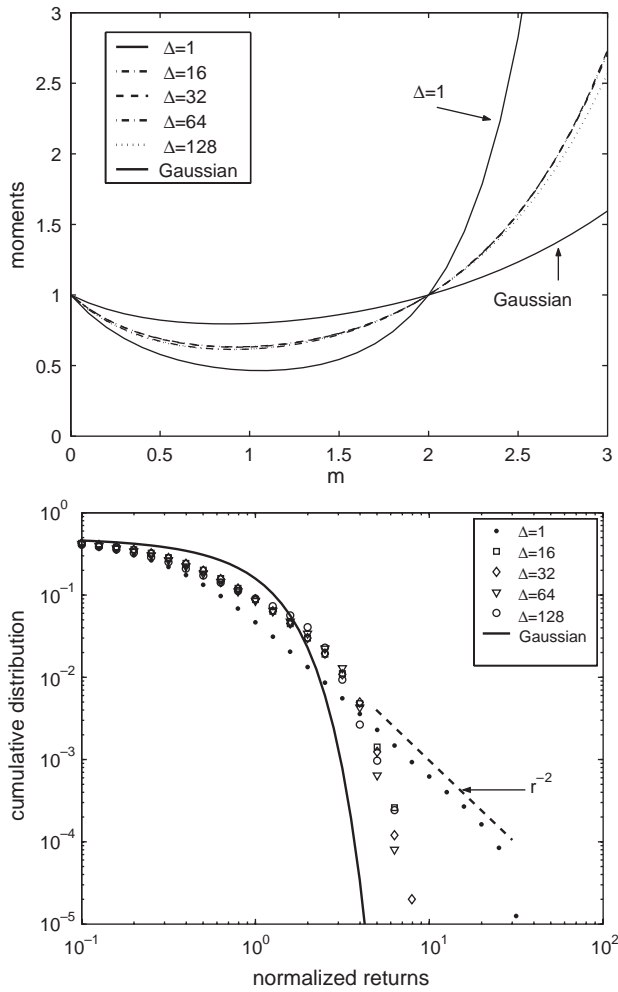


Fig. 8. (a) Moments of the normalized returns, for lag times $\Delta = 1, 16, 32, 64,$ and 128 min. (b) Corresponding cumulative distribution functions, with the dashed line showing a power-law with exponent -2 .

normalized returns are defined by dividing by the volatility:

$$g_{\Delta}(t) = \frac{r_{\Delta}(t)}{\text{vol}(\Delta)}, \tag{67}$$

and the moments

$$\langle |g_{\Delta}(t)|^m \rangle \tag{68}$$

of the numerical simulations are plotted in Fig. 8(a) as a function of m , for lags of 1, 16, 32, 64, and 128 min. The extremely non-Gaussian distribution at $\Delta = 1$ min relaxes to a shape which remains stable up to $\Delta \approx 128$ min—note the moments for

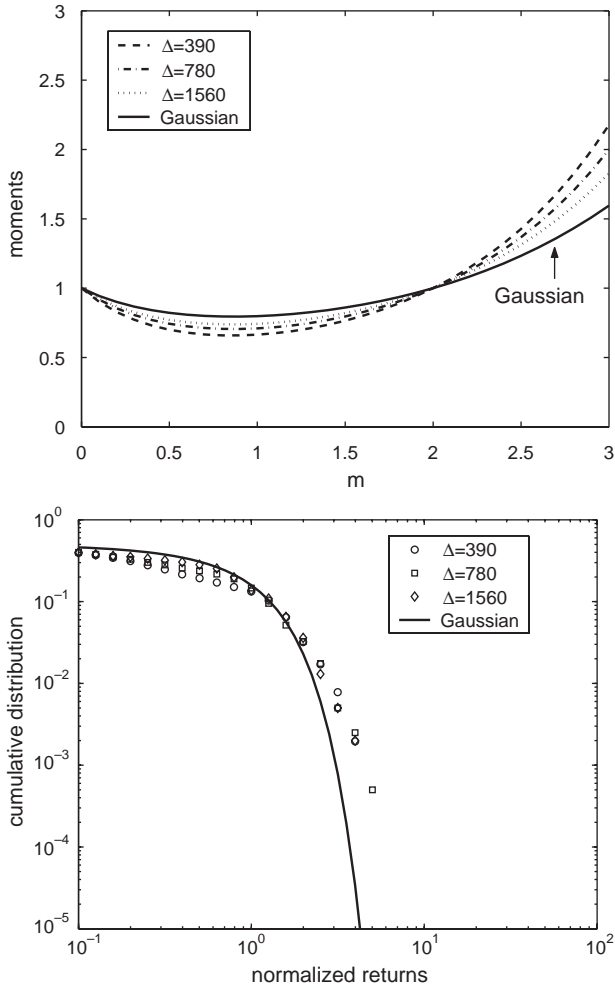


Fig. 9. (a) Moments of the normalized returns, for lag times $\Delta = 390, 780,$ and 1560 min. (b) Corresponding cumulative distribution functions.

lags from 16 to 128 min are almost indistinguishable in Fig. 8(a). This conclusion is supported by the cumulative distribution of the normalized returns shown in Fig. 8(b). This is very similar to the behavior observed in empirical data, see Fig. 6 of Ref. [6], although the model does not produce power-law scaling of the distribution tails (except for the region with exponent -2 for lag $\Delta = 1$ min). The returns distributions eventually converge to a Gaussian distribution, see the corresponding plots for lags of 390, 780, and 1560 min (1 to 4 trading days) in Fig. 9. This convergence to Gaussian is somewhat faster than observed in the S&P500 in Ref. [6], where non-Gaussian moments and cumulative distributions persist until approximately 4 days. Our corresponding estimate for the model persistence time (based

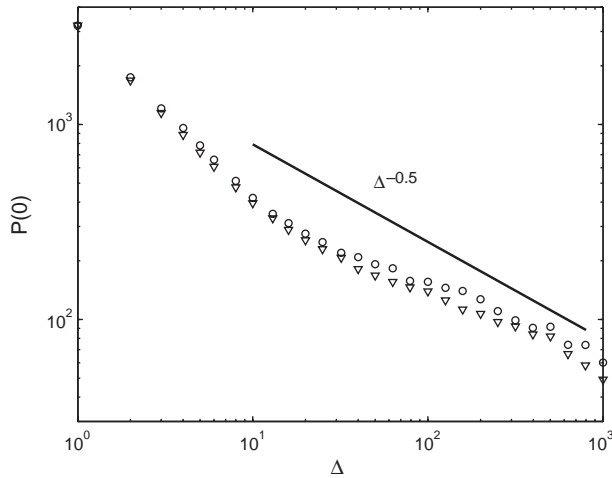


Fig. 10. Scaling of the peak $P(0)$ of the stock returns PDF with lag time Δ . Solid line shows a Gaussian scaling, with exponent -0.5 .

on the moments in Fig. 8(a)) is 128 min, an order of magnitude smaller than the S&P500 value.

The scaling of the peak $P(0)$ of the PDF of *stock price returns* $S(t + \Delta) - S(t)$ was examined in Ref. [5] for S&P500 data. A power-law scaling of $P(0)$ with lag was discovered, with exponent -0.7 . In Fig. 10 we mimic this study, generating the time series $S(t)$ from $x(t)$ in order to calculate the stock price return. Results are shown from two separate realizations, along with a line indicating Gaussian scaling of exponent $-\frac{1}{2}$. It is clear that, unlike the S&P500 returns, the model $P(0)$ does not scale as a single power-law with Δ , although it appears to approach the Gaussian scaling at the highest lags.

6.1. Options pricing

An important test for any model of market dynamics is its usefulness in pricing options [32]. Let C denote the price at time $t = 0$ of a European call option with date of maturity T and strike price K . The price of the underlying instrument is $S(t)$ at time t , and a corresponding log-price is defined as in Eq. (1). At time T , the owner of the option receives the payout

$$\max[S(T) - K, 0], \tag{69}$$

and the price of the option at time $t = 0$ is therefore [31]

$$C = \langle e^{-rT} \max[S(T) - K, 0] \rangle, \tag{70}$$

where r is the interest rate, and the averaging is over the risk-neutral probability density. The option price may be written as an integral over the PDF $\theta(x)$ of the

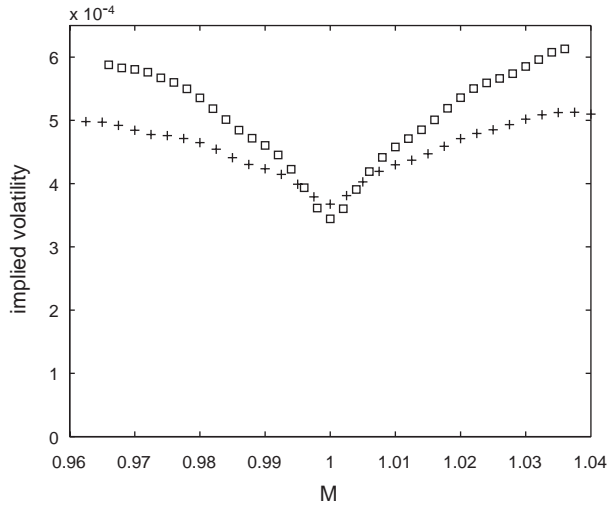


Fig. 11. Volatility smiles for European call option calculated by numerical simulation of the paths (62), with $k = 500$ and interest rate $r = 0$. Smiles for two times to maturity T are shown: $T = 390$ min (squares) and $T = 1000$ min (crosses).

log-price as

$$\frac{C}{K} = e^{-rT} \int_{-\ln M}^{\infty} (Me^x - 1)\theta(x) dx, \tag{71}$$

where the ratio $M = S(0)/K$ has been introduced; M is called the *moneyness* of the option [32]. (Note that Carmona and Durrleman [31] instead define the moneyness as Me^{rT}). Given an evolution equation for the log-price $x(t)$, the integral in (71) may be approximated by a Monte Carlo computation over the endpoints $x(T)$ of the log-price sample paths. If the PDF $\theta(x)$ is known in closed form, the option price may be calculated exactly from (71). For example, price dynamics governed by the standard random walk model (2) lead to a Gaussian PDF for x , and so to the well-known Black–Scholes formula for C :

$$\frac{C}{K} = M\Phi(d_1) - e^{-rT}\Phi(d_2), \tag{72}$$

with

$$d_1 = \frac{\ln(Me^{rT})}{\sigma\sqrt{T}} + \frac{1}{2}\sigma\sqrt{T}, \quad d_2 = d_1 - \sigma\sqrt{T}, \tag{73}$$

and

$$\Phi(y) = \frac{1}{\sqrt{2\pi}} \int_{-\infty}^y e^{-z^2/2} dz. \tag{74}$$

The quantity σ appearing in this formula is the Black–Scholes volatility, i.e., it appears in the PDF $\theta(x)$ such that the variance of x is $\sigma^2 T$. For a given time to maturity T , and interest rate r , it is thus possible to calculate the option price on an instrument in our random field model by numerical simulation, and to compare to the price given by the Black–Scholes formula (72) for a variety of moneyness ratios M . Our results (Fig. 11) are presented in terms of an implied volatility [3], i.e., the value σ for which the Black–Scholes price (72) equals the price found by Monte Carlo simulation. Because the returns distributions in the random field model are non-Gaussian, the implied volatility varies with M , being lowest at the money ($M = 1$), and increasing for options which are either in the money ($M > 1$) or out of the money ($M < 1$). The shape of the curve in Fig. 11 is similar to that observed in markets, where it is referred to as the ‘volatility smile’ [3].

7. Conclusion

We have proposed a new model for the fluctuations of stock prices, in which the rate of change of the log price is randomly dependent upon both time and the current price, see Eq. (7). This is a very general modelling concept, with the attractive feature that Gaussian Eulerian fields may give non-Gaussian Lagrangian statistics in the observable data, i.e., the time series of returns. Moreover, random field models can be derived from some simple assumptions on the behavior of trading agents (Section 2.1). As noted in Section 5, Monte Carlo simulations of Eq. (7) can be used to find the model predictions for any random field. In this paper we focus on a special case, the $\varepsilon \rightarrow 0$ limit of a single-scale random field, for which exact analytical results are obtainable, and for which numerical simulations are particularly efficient.

Our main analytical results are the expression (48) for the Lagrangian velocity correlation $L(t)$ in terms of the given Eulerian field correlation $R(t)$, and the quadrature formulas (40) and (52) giving the correlation function and volatility of the returns. Numerical simulations of stock price time series are efficiently performed using Eq. (62), and allow us to examine features not amenable to exact analysis.

We find that several of the important empirical stylized facts (i)–(iv) listed in the Introduction are reproduced by our model, using the correlation function (61) for computational convenience. The parameter values k and T are chosen by comparing the model’s volatility to the data in Fig. 3(c) of Ref. [6]. With reference to the stylized facts listed in Section 1, the results of the single-scale random field model may be summarized as follows.

- (i) Model returns are non-Gaussian, with fat tails and the center of the distribution well-fitted by the Lévy distribution used in Ref. [5]. The tails of the cumulative distributions of model returns do not, however, have the power-law scaling found in Ref. [6]. The normalized model returns distributions exhibit a slow return toward Gaussian, on timescales an order of magnitude longer than the characteristic time of $R(t)$. However, these timescales are an order of magnitude smaller those found for the convergence to Gaussian in the S&P500 returns in Ref. [6].

- (ii) The correlation function of model returns decays quickly (similar to exponentially) over a short timescale. Following the fast decay, the correlation becomes negative, with magnitude decaying more slowly to zero. Although the fast decay for lags under 10 min is very similar that found for the S&P500 in Ref. [6], the empirical correlation function does not reach negative values, rather remaining at a constant “noise level”. Whether this noise level could be masking negative correlation values as predicted by the model is a question requiring further extensive analysis of market data.
- (iii) The volatility of the model returns grows diffusively for lag times longer than 10 min. The super-diffusive volatility at higher frequencies (shorter lags) is actually due to a logarithmic correction to power-law growth (53), but for the range of lags examined in Refs. [6,7] it matches well to a super-diffusive power-law. Higher frequency data is needed to determine which form best fits the actual stock market volatility.
- (iv) Our model does not have a simple scaling of $P(0)$ with lag, in contrast to the case of S&P500 prices as demonstrated in Fig. 1 of Ref. [5].

In summary, the single-scale random field model yields time series which have many (but not all) of the important properties of empirical data. The model gives an appealingly intuitive picture of the causes of non-Gaussian behavior in markets, and provides a simple algorithm for generating time series with many market-like features. We anticipate that this algorithm will prove particularly useful in Monte Carlo simulations to determine prices of options and derivatives, as demonstrated in Section 6.1.

The concept of modelling stock prices by motion in a random field is quite general—our restriction in this paper to the single-scale case is purely because of the existence of analytical results in this case. It would be very interesting to determine the sensitivity of the results obtained here to the form of the random field. As shown in Fig. 2, the small- ε limit of non-single-scale fields again leads to motion along the $u = 0$ contours, but may also include fast jumps in stock prices. We anticipate that the results presented here will be largely applicable to the contour-following motion in more general fields, but further work is required to describe the statistics of the jumps in stock price. Further work is also in progress to investigate the dependence of all results on finite values of ε , using numerical simulations of Eq. (7).

Acknowledgements

The author gratefully acknowledges helpful discussions with John Appleby and Paul O’Gorman. This work is supported by funding from a Science Foundation Ireland Investigator Award 02/IN.1/IM062, and from the Faculty of Arts Research Fund, University College Cork.

References

- [1] L. Bachelier, *Ann. Sci. Ec. Norm. Sup.* 3 (1900) 21.
- [2] P.A. Samuelson, in: P.H. Cootner (Ed.), *The Random Character of Stock Market Prices*, MIT Press, Cambridge, 1964, p. 506.
- [3] J.C. Hull, *Options, Futures, and Other Derivatives*, Prentice-Hall, London, 2003.
- [4] J.Y. Campbell, et al., *The Econometrics of Financial Markets*, Princeton University Press, Princeton, 1997.
- [5] R.N. Mantegna, H.E. Stanley, *Nature* 376 (1995) 46.
- [6] P. Gopikrishnan, et al., *Phys. Rev. E* 60 (1999) 5305.
- [7] J. Masoliver, M. Montero, J.M. Porrà, *Physica A* 283 (2000) 559.
- [8] N.G. Van Kampen, *Stochastic Processes in Physics and Chemistry*, Elsevier, Amsterdam, 1992.
- [9] L. Arnold, *Stochastic Differential Equations: Theory and Applications*, Wiley, New York, 1974.
- [10] B.B. Mandelbrot, *J. Bus.* 36 (1963) 394.
- [11] R.N. Mantegna, H.E. Stanley, *Phys. Rev. Lett.* 73 (1994) 2946.
- [12] R.F. Engle, *Econometrica* 50 (1982) 987.
- [13] T. Bollerslev, R.Y. Chou, K.F. Kroner, *J. Econom.* 52 (1992) 5.
- [14] O.E. Barndorff-Nielsen, N. Shephard, *J. R. Statist. Soc. B* 63 (2001) 167.
- [15] J. Masoliver, M. Montero, G.H. Weiss, *Phys. Rev. E* 67 (2003) 021112.
- [16] R.N. Mantegna, H.E. Stanley, *Physica A* 254 (1998) 77.
- [17] R.N. Mantegna, H.E. Stanley, *Physica A* 274 (1999) 216.
- [18] J.P. Gleeson, D.I. Pullin, *Phys. Fluids* 15 (2003) 3546.
- [19] J.B. Witkoskie, S. Yang, J. Cao, *Phys. Rev. E* 66 (2002) 051111.
- [20] A.M. Balk, *J. Fluid Mech.* 467 (2002) 163.
- [21] R.H. Kraichnan, *Phys. Fluids* 13 (1970) 22.
- [22] W.D. McComb, *The Physics of Fluid Turbulence*, Oxford University Press, Oxford, 1990.
- [23] C.L. Zirbel, *Adv. Appl. Prob.* 33 (2001) 810.
- [24] M. Vlad, et al., *Phys. Rev. E* 63 (2001) 066304.
- [25] J.P. Gleeson, *Phys. Rev. E* 66 (2002) 038301.
- [26] Y. Liu, et al., *Phys. Rev. E* 60 (1999) 1390.
- [27] R.E. O'Malley, *Singular Perturbation Methods for Ordinary Differential Equations*, Springer, New York, 1991.
- [28] J.P. Gleeson, *Phys. Rev. E* 65 (2002) 037103.
- [29] J.M. Ziman, *Models of Disorder*, Cambridge University Press, Cambridge, 1979.
- [30] A.J. Majda, P.R. Kramer, *Phys. Rep.* 314 (1999) 237.
- [31] R. Carmona, V. Durrleman, *SIAM Rev.* 45 (2003) 627–685.
- [32] J. Perello, J. Masoliver, *Physica A* 308 (2002) 420–442.